

## Long-range antiferromagnetic order of formally nonmagnetic $\text{Eu}^{3+}$ Van Vleck ions observed in multiferroic $\text{Eu}_{1-x}\text{Y}_x\text{MnO}_3$

A. Skaugen,<sup>1</sup> E. Schierle,<sup>2</sup> G. van der Laan,<sup>3</sup> D. K. Shukla,<sup>1,4</sup> H. C. Walker,<sup>1,5</sup> E. Weschke,<sup>2</sup> and J. Stropfer<sup>1,\*</sup>

<sup>1</sup>Deutsches Elektronen-Synchrotron DESY, Notkestraße 85, D-22607 Hamburg, Germany

<sup>2</sup>Helmholtz-Zentrum Berlin für Materialien und Energie, Albert-Einstein-Str. 15, D-12489 Berlin, Germany

<sup>3</sup>Diamond Light Source, Chilton, Didcot OX11 0DE, United Kingdom

<sup>4</sup>UGC DAE Consortium for Scientific Research, Khandwa Road, Indore 01, India

<sup>5</sup>ISIS, Rutherford Appleton Laboratory, Chilton, Didcot OX11 0QX, United Kingdom

(Received 26 July 2014; revised manuscript received 22 April 2015; published 27 May 2015)

We report on resonant magnetic x-ray scattering and absorption spectroscopy studies of exchange-coupled antiferromagnetic ordering of  $\text{Eu}^{3+}$  magnetic moments in multiferroic  $\text{Eu}_{1-x}\text{Y}_x\text{MnO}_3$  in the absence of an external magnetic field. The observed resonant spectrum is characteristic of a magnetically ordered  ${}^7F_1$  state that mirrors the Mn magnetic ordering, due to exchange coupling between the Eu  $4f$  and Mn  $3d$  spins. Here, we observe long-range magnetic order generated by exchange coupling of magnetic moments of formally nonmagnetic Van Vleck ions, which is a step further towards the realization of exotic phases induced by exchange coupling in systems entirely composed of non magnetic ions.

DOI: [10.1103/PhysRevB.91.180409](https://doi.org/10.1103/PhysRevB.91.180409)

PACS number(s): 75.25.-j, 75.47.Lx, 75.50.Ee, 75.85.+t

The interplay between local spin and orbital magnetic moments is an important factor in a large variety of magnetic ordering phenomena exploited in present day applications. In special cases, even with magnetic moments present, a system can form a nonmagnetic singlet ground state. Prominent examples are rare-earth and transition-metal ions with the  $f$  or  $d$  shell missing one electron for half filling. Here the orbital and spin moments can cancel out generating a  $J = 0$  ground state. However, having only a small energy spacing between the ground state and the first magnetic triplet state, magnetism can in such systems be generated by symmetry breaking external stimuli such as magnetic or electric fields. In the case of magnetic stimulus this is known as Van Vleck magnetism and offers fascinating possibilities for new applications, for example for a magnetic sensor that is itself nonmagnetic. From a more fundamental point of view such systems are candidates for a variety of novel states of matter characterized by hidden order [1], Bose-Einstein condensation, or quantum phase transitions [2,3].

A paramount example of a formally nonmagnetic ion being susceptible to external magnetic fields is the  $\text{Eu}^{3+}$  ion with  $S = 3$  and  $L = 3$ , having a  $J = 0$  nonmagnetic ground state. Van Vleck magnetism has long been known to contribute to the paramagnetic moment of  $\text{Eu}^{3+}$  [4–7]. For this ion, the symmetry breaking by an external magnetic field mixes the  ${}^7F_1$  state into the ground state, yielding a finite magnetic moment. A more recent example of this mechanism is the observation of x-ray magnetic circular dichroism (XMCD) in  $\text{EuN}$  under an applied magnetic field of 5 T, which is explained by magnetic field induced admixture of  ${}^7F_1$  into the  ${}^7F_0$  ground state [8]. The possibility of spin ordering without external electric or magnetic stimulus in the case of a vanishing total magnetic moment has been discussed theoretically, setting up the possibility of an unconventional phase transition in which the spin correlation length diverges but there is little or no change in the magnetic properties [9].

While these previous studies revealed the presence of Van Vleck magnetic moments, experimental proof of intrinsic long-range magnetic order of Van Vleck ions is missing. The perovskite-structure rare-earth (RE) manganites  $\text{RMnO}_3$  are well-suited candidates to show such a mechanism. These compounds have attracted much attention due to their strong magnetoelectric effect and the possibility to control electric (magnetic) order by magnetic (electric) fields [10–13]. These multiferroic properties are largely related to the magnetic order of the Mn  $3d$  magnetic moments [14,15]. However, RE magnetic ordering has been shown to play a decisive role in the multiferroicity of these compounds in past years [16–20]. In systematic studies of such complex compounds, a standard way to disentangle various magnetic contributions is the comparison with a compound involving a nonmagnetic RE. In multiferroics, the  $\text{Eu}_{1-x}\text{Y}_x\text{MnO}_3$  series of compounds is a prominent example [15,21,22]. The  $J = 0$  ground state of  $\text{Eu}^{3+}$  is nonmagnetic and has spherical symmetry, so the crystal field splitting is expected to be small. However, exchange coupling between Mn  $3d$  and RE  $4f$  states is an interaction between spins and does not involve the orbital moment  $L$ , and may hence induce a Van Vleck  $J = 1$  magnetic moment in  $\text{Eu}^{3+}$ . As a consequence,  $\text{Eu}^{3+}$  might not be anticipated as a completely nonmagnetic reference ion in exchange-coupled materials, but displays a perfect candidature for magnetic order originating from Van Vleck magnetism.

In this Rapid Communication, we demonstrate long-range complex antiferromagnetic order of  $\text{Eu}^{3+}$  ions without invoking an external electromagnetic field or macroscopic magnetization. We used resonant elastic x-ray scattering (REXS) to study the magnetic reflections from  $\text{Eu}_{0.8}\text{Y}_{0.2}\text{MnO}_3$ . REXS is particularly suited for this purpose by virtue of element specificity, high sensitivity to detect even weak antiferromagnetic ordering of Eu  $4f$  moments, and spectroscopic information for identifying the  $J$  state involved in the ordering.

The soft x-ray experiments were carried out using the XUV diffractometer and the high-field diffractometer at beamline UE46-PGM1 at the BESSY II storage ring [23,24], while the

\*joerg.stropfer@desy.de

hard x-ray data were taken at beamline P09 at the PETRA III storage ring at DESY [25]. The scattering experiments at both facilities were carried out in horizontal scattering geometry from the polished  $b$  surface of the sample [26], at PETRA III with  $a$  perpendicular to the scattering plane, and at BESSY II with  $c$  perpendicular to the scattering plane, unless otherwise noted. For cooling the sample, a 14 T cryomagnet and a Displex cryostat were used at P09, and a continuous flow LHe cryostat was used at UE46-PGM1. For the hard x-ray experiments a Cu (220) polarization analyzer was mounted behind the sample to separate the  $\pi$ - $\pi'$  and  $\pi$ - $\sigma'$  channels and to suppress the fluorescence background. Here  $\pi$  ( $\pi'$ ) and  $\sigma$  ( $\sigma'$ ) denote polarization directions of the incoming (outgoing) beam parallel and perpendicular to the scattering plane, respectively [27]. At BESSY II the incident polarization was varied, and the total scattered beam was detected.

The Mn magnetic structure of  $\text{Eu}_{3/4}\text{Y}_{1/4}\text{MnO}_3$  below  $T_C \approx 28$  K has been shown to consist of an  $A$  type  $ab$ -plane cycloid with a wave vector  $\tau = \frac{1}{4}\mathbf{b}^*$  in the  $Pbnm$  orthorhombic unit cell, upon which an  $F$  type  $c$ -axis sinusoid is superposed through the Dzyaloshinskii-Moriya interaction [28]. The same mechanism is also expected to induce a  $G$  type  $ab$ -plane cycloid and a  $C$  type  $c$ -axis sinusoid.  $\text{Eu}_{0.8}\text{Y}_{0.2}\text{MnO}_3$  was investigated at low temperature in the ferroelectric phase. Measuring the REXS intensity at the Mn  $K$  edge, magnetic  $A$ ,  $F$ ,  $G$ , and  $C$  type reflections were observed. For the  $C$  type reflection at the Mn  $K$  edge, a very weak signal was found in the  $\pi$ - $\sigma'$  channel only, which indicates that the Mn moments are oriented along  $c$ . In contrast, at the Mn  $L_{2,3}$  edges only the  $F$  type reflection is accessible within the limited size of the Ewald sphere at this photon energy.

Remarkably, intense resonant  $F$  and  $C$  type reflections could be observed at the Eu  $M_{4,5}$  edges as well. The resonant behavior at the  $\text{Eu}^{3+}$   $M_{4,5}$  absorption edges is demonstrated in Fig. 1. The inset of Fig. 1(a) shows a reciprocal space scan over the  $C$  type  $(0\ 1 - \tau\ 0)$  reflection at  $T = 10$  K with  $\pi$  and  $\sigma$  incident polarization, respectively, and the photon energy tuned to 1127 eV, close to the Eu  $M_5$  absorption edge. The absence of intensity for  $\sigma$  incident light indicates that this reflection is caused by magnetic scattering from the formally nonmagnetic  $\text{Eu}^{3+}$  ions with the corresponding moments pointing along the  $c$  direction, i.e., moments parallel to the Mn moments as observed at the Mn  $K$ -edge resonance. Resonant enhancement at formally nonmagnetic anions has been observed in earlier studies and mainly been attributed to transferred moments in hybrid orbitals [29–31]. In contrast to all former observations, however, the Van Vleck ion  $\text{Eu}^{3+}$  has the possibility to create a magnetic moment in the corelike  $4f$  shell by populating the magnetic  ${}^7F_1$  excited state. The photon energy dependence of the  $C$  type magnetic reflection is shown in Fig. 1(a), and can be readily explained by considering the resonant magneto-optical parameters connected with a  ${}^7F_1$  state. The expected line shape is calculated on the basis of experimental XMCD data [8] of paramagnetic  $\text{Eu}^{3+}$  and invoking a Kramers-Kronig transform [32]; the result is shown as a red curve in Fig. 1(a). Comparison to the measured REXS line shape (blue curve) yields a good match, apart from a relative difference in intensities between the  $M_4$  and  $M_5$  edges and a small offset in photon energy. This result shows that the peak observed at the Eu  $M_{4,5}$  edges is indeed of magnetic origin

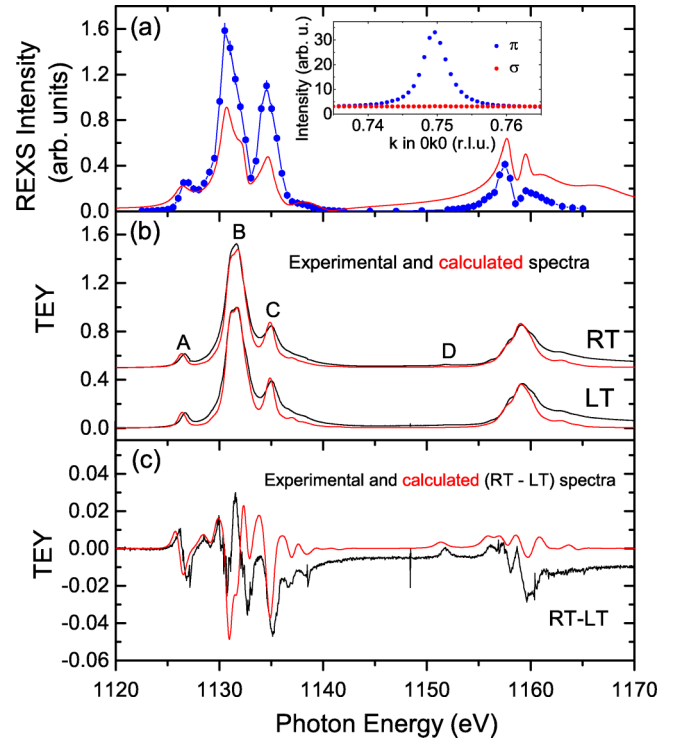


FIG. 1. (Color online) (a) Absorption corrected REXS spectrum [blue (dark gray) curve] of  $(0\ 1 - \tau\ 0)$  across the Eu  $M_5$  and  $M_4$  edges at  $T = 10$  K, and line shape calculation [red (light gray) curve] based on the XMCD spectrum from Ref. [8]. The inset shows reciprocal space scans of the reflection for  $\pi$  and  $\sigma$  incident polarization. (b) Experimental TEY spectra and multiplet calculations at  $T = 296$  K (RT) and  $T = 120$  K (LT). (c) Measured and calculated difference between high and low temperature spectra.

caused by a populated  ${}^7F_1$  state. To clarify the mechanism populating the  ${}^7F_1$  state we performed x-ray absorption spectroscopy at different temperatures by measuring the total electron yield (TEY) [Fig. 1(b)]. We then compared the TEY data to single ion atomic multiplet calculations of the relevant electronic states [33].

Figure 1(b) shows the x-ray absorption spectra across the Eu  $M_{4,5}$  edges at two different temperatures, 296 K (RT) and 120 K (LT). The spectra are normalized such that the integrated intensity of the difference spectrum in Fig. 1(c) is perceived to be as small as possible. Due to the sample being ferroelectric and thus insulating at low temperatures, 120 K was the lowest temperature we were able to measure TEY spectra without encountering charge buildup on the surface.

These spectra are compared to multiplet calculations  $4f^6 \rightarrow 3d^9 4f^7$ , performed assuming Boltzmann population of the different  $J$  levels. The calculations result in 26.9% and 1.7%  ${}^7F_1$  population at RT and LT, respectively, as expected from the thermal population ( $E_{J=1} - E_{J=0} = 53$  meV). There are some striking differences between the RT and LT spectra seen in the experiment which are fully confirmed by the calculation: The peaks A, C, and the low-energy shoulder of the main peak B are all lower for RT, and a small additional peak D appears for RT. Altogether, there is an excellent agreement between experiment and calculation for the (RT-LT) difference

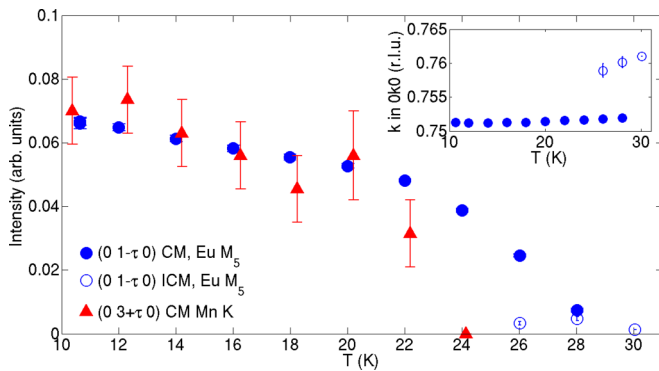


FIG. 2. (Color online) Temperature dependence of the integrated intensity of the  $C$  type  $(0\ 1 - \tau\ 0)$  reflection at the Eu  $M_5$  resonance (blue circles). Red triangles show the  $T$  dependence of the  $C$  type  $(0\ 3 + \tau\ 0)$  reflection at the Mn  $K$  edge. The data have been scaled to fit onto the same plot. The inset shows the peak positions in  $q$  space over the same temperature range.

spectra shown in Fig. 1(c), taking into account some small peak shifts, asymmetric line shapes, and continuum background not included in the calculation. Furthermore, the magnitudes of the experimental and calculated differences are in good agreement with each other. The maximum difference is  $\sim 5\%$ . The magnitude of the difference spectrum scales with the percentage of higher  $J$  population. Thus the thermal population of  $J \neq 0$  states cannot explain the resonant signal at 10 K. The analysis puts an upper limit of  $\sim 10\%$  to a temperature-independent  ${}^7F_1$  contribution, i.e., from hybridization and crystal field effects.

The negligible influence of the temperature on the  ${}^7F_1$  population is also reflected in the observed temperature-dependent peak intensity. The temperature dependence of the  $C$  type reflection  $(0\ 1 - \tau\ 0)$  was measured both at the Mn  $K$  edge and at the Eu  $M_5$  edge, and is shown in Fig. 2. Apart from smaller error bars for the much stronger signal at the Eu  $M_5$  absorption edge, we observe a perfect match of the temperature-dependent peak intensities, disappearing at the transition into the paraelectric phase. This behavior is in accordance with the proposed magnetic structure; the behavior of the  $\text{Eu}^{3+}$  ions, in particular, reflects that of the corresponding order parameter. This demonstrates a strong coupling between the Mn and the  $\text{Eu}^{3+}$  magnetic order capable of breaking the symmetry of the  $4f$  wave function.

The stronger signal at the Eu  $M_5$  resonance reveals a second incommensurate structure close to the transition into the paraelectric phase, with a temperature-dependent peak position as shown in the inset of Fig. 2. This is also found in respective data recorded at the Eu  $L_{2,3}$  edges, where in addition,  $A$ ,  $C$ ,  $F$ , and  $G$  type reflections were also observed. While  $C$  and  $F$  type order are expected to polarize the induced  $\text{Eu}^{3+}$  moments in this compound, the observation of  $A$  and  $G$  type Eu order is more surprising, since Eu in the  $Pbnm$  space group sits at the crystallographic mirror perpendicular to the  $c$  axis. This means that the exchange field from the  $A$  and  $G$  type Mn order, both being antiferromagnetically ordered along  $c$ , would cancel out at the Eu site, and  $A$  and  $G$  type order of the  ${}^7F_1$  moments can in theory not be induced. However, similar observations have also been made in earlier studies on  $\text{TbMnO}_3$ , where the Tb moments

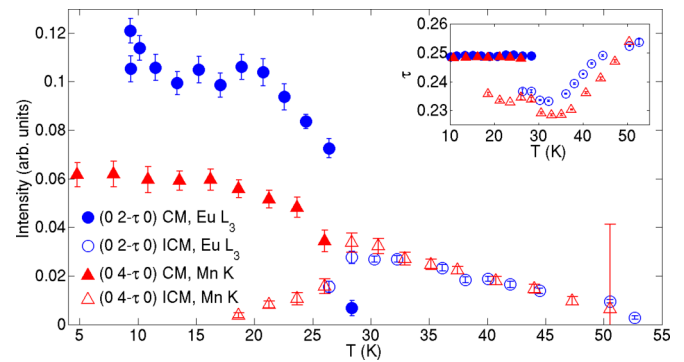


FIG. 3. (Color online) Temperature dependence of the integrated intensity of the  $F$  type  $(0\ 2 - \tau\ 0)$  reflection at the Eu  $L_3$  absorption edge (blue circles). The inset shows the peak positions in  $q$  space in the same temperature range. Red triangles show the temperature dependence of the  $F$  type  $(0\ 4 - \tau\ 0)$  reflection at the Mn  $K$  edge. The data have been scaled to fit onto the same plot.

mirror the  $A$  type Mn magnetic structure in the collinear phase [34,35]. Possible explanations, already discussed in the above-mentioned references, are either a nonmagnetic origin of these reflections, or ionic displacements of the Eu ions from their ideal positions which could either lift the strict extinction rules for the  $A$  and  $G$  type reflections or even break the crystal symmetry such that  $A$  and  $G$  type order can be induced at the Eu sites. As known from other  $\text{RMnO}_3$  compounds, varying amounts of frustration are introduced to the crystal structure by substituting in rare-earth ions with different ionic radii. It is therefore reasonable to expect that the  $Pbnm$  symmetry in the current sample might be broken such that the Eu is no longer located exactly on a crystallographic mirror. Our data are fully consistent with such a scenario, making a nonmagnetic origin rather less likely. However, if ionic displacement of the Eu ions is the correct explanation, our data do not allow the identification of the type of ionic displacement or the driving mechanism behind it.

Since the resonant signal at the Eu  $L_{2,3}$  edges does not directly probe the  $4f$  states, but rather the  $5d$  electrons, we do not gain a noteworthy signal enhancement compared to the Mn  $K$ -edge resonance for these reflections. Nonetheless, it allows the comparison of all the relevant reflections from  $\text{Eu}^{3+}$  with those observed at the Mn  $K$  edge. Figure 3 shows the integrated intensities of the  $F$  type reflections  $(0\ 2 - \tau\ 0)$  and  $(0\ 4 - \tau\ 0)$  as functions of temperature at the Eu  $L_3$  and Mn  $K$  absorption edges, respectively. The commensurate (CM) and incommensurate (ICM) phases are recognized in both temperature spectra, and match the phase transitions observed elsewhere [21,22,26]. The only major difference in the data is the relative difference in intensity between the CM and the ICM reflections, being slightly larger at the Eu  $L_3$  edge.

We thus observe a common behavior of the magnetic reflections both at the Mn  $K$  edge and the Eu absorption edges when it comes to the intensity and  $\mathbf{q}$  dependence with varying temperature and photon polarization, along with an order parameter-like behavior of the Eu magnetic order. Hence the Eu resonant reflections are caused by magnetic order of the  $\text{Eu}^{3+}$   ${}^7F_1$  moments which mirrors the magnetic structure of Mn moments. The  ${}^7F_1$  state of  $\text{Eu}^{3+}$  can be induced by several symmetry breaking mechanisms, of which two present

themselves as the most likely. The fact that the Eu moments mirror the Mn magnetic structure clearly shows the presence of an exchange field at the Eu sites. This exchange field will cause a local symmetry breaking at the Eu sites that, like the symmetry breaking by an external magnetic field, can result in a population of the  ${}^7F_1$  state. In a similar way, a local symmetry breaking due to the crystal field could also populate the  ${}^7F_1$  excited state, i.e., an electric field could transform the nonmagnetic ion into a magnetic one. Whether the symmetry is broken primarily by the crystal field or the Mn exchange field, the populated  ${}^7F_1$  state at the Eu sites is exchange coupled to the Mn magnetic sublattice. In principle, this scenario also allows for Eu-Eu exchange interaction [36]. The mechanism here is very different from the origin of the magnetic polarization observed at oxygen sites in similar multiferroics, which is caused by spin-dependent hybridization [30,31].

The existence of a nonzero Eu magnetic moment in  $\text{Eu}_{0.8}\text{Y}_{0.2}\text{MnO}_3$  raises a couple of issues. First, it puts into question the assumption of  $\text{Eu}_{1-x}\text{Y}_x\text{MnO}_3$  being a model system for multiferroic orthomanganites free from RE magnetism. As soon as the magnetic Eu state is induced, Eu-Mn and Eu-Eu exchange coupling as well as Eu magnetic anisotropy can contribute to the magnetic order of the entire system with the possibility of an indirect impact on the field-dependent multiferroicity. Furthermore, similar RE magnetic structures have been shown to contribute directly to ferroelectricity in  $\text{RMnO}_3$  ( $R = \text{Tb, Dy, Gd}$ ) by symmetric exchange striction mechanisms [14,16–18,20,37–39].

Secondly, the discovery of a Eu magnetic moment without self-ordering opens up the possibility of using Eu as a magnetic probe. As seen in Fig. 2, by making use of the strong resonant

enhancement at the Eu  $M_{4,5}$  edges we gain a drastically stronger signal from which we are able to extract intensities and  $q$  values to much higher precision than what is possible at the Mn  $K$  edge. The onset of the ferroelectric phase below  $\sim 28$  K is clearly seen. Measuring at the Eu  $M_{4,5}$  edges also has the added benefit of being able to explore a larger Ewald sphere compared to the Mn  $L_{2,3}$  edges, where detailed studies of Mn magnetism are usually performed.

Thirdly, our findings may have implications for magnetism in other transition metals. Van Vleck effects are expected to appear in Eu, but not in  $3d$  transition metals, where the orbital moment is usually quenched. There are, however, Van Vleck materials where exchange coupling plays a role and antiferromagnetic order in a field is associated with Bose-Einstein condensation of magnons [3]. More significantly, the increasing spin-orbit interaction in  $4d$  and  $5d$  transition metals renders Van Vleck effects more important in this class of materials that are increasingly attracting interest [40].

In conclusion, we have presented an observation of long-range antiferromagnetic order of Van Vleck ions, where the ordering is due to exchange coupling between Eu and Mn spins. Since an exchange interaction between  $\text{Eu}^{3+}$   $4f$  moments could already, in principle, intermix  ${}^7F_1$  contributions, our observation allows for the hope to observe complex long-range magnetic order in systems consisting entirely of formally nonmagnetic ions, where novel properties may be expected.

Parts of this research were carried out at the light source PETRA III at DESY and the light source BESSY II at Helmholtz Center Berlin, both members of the Helmholtz Association (HGF).

- 
- [1] H. Adachi and H. Ino, *Nature (London)* **401**, 148 (1999).
- [2] C. Ruegg, N. Cavadini, A. Furrer, H.-U. Gudel, K. Kramer, H. Mutka, A. Wildes, K. Habicht, and P. Vorderwisch, *Nature (London)* **423**, 62 (2003).
- [3] V. S. Zapf, D. Zocco, B. R. Hansen, M. Jaime, N. Harrison, C. D. Batista, M. Kenzelmann, C. Niedermayer, A. Lacerda, and A. Paduan-Filho, *Phys. Rev. Lett.* **96**, 077204 (2006).
- [4] A. Frank, *Phys. Rev.* **39**, 119 (1932).
- [5] J. H. Van Vleck, *J. Appl. Phys.* **39**, 365 (1968).
- [6] M. S. Tagirov and D. A. Tayurskii, *Low Temp. Phys.* **28**, 147 (2002).
- [7] Y. Takikawa, S. Ebisu, and S. Nagata, *J. Phys. Chem. Solids* **71**, 1592 (2010).
- [8] B. J. Ruck, H. J. Trodahl, J. H. Richter, J. C. Cezar, F. Wilhelm, A. Rogalev, V. N. Antonov, B. D. Le, and C. Meyer, *Phys. Rev. B* **83**, 174404 (2011).
- [9] M. D. Johannes and W. E. Pickett, *Phys. Rev. B* **72**, 195116 (2005).
- [10] M. Fiebig, *J. Phys. D* **38**, R123 (2005).
- [11] T. Kimura, T. Goto, H. Shintani, K. Ishizaka, T. Arima, and Y. Tokura, *Nature (London)* **426**, 55 (2003).
- [12] T. Goto, T. Kimura, G. Lawes, A. P. Ramirez, and Y. Tokura, *Phys. Rev. Lett.* **92**, 257201 (2004).
- [13] T. Kimura, G. Lawes, T. Goto, Y. Tokura, and A. P. Ramirez, *Phys. Rev. B* **71**, 224425 (2005).
- [14] M. Mostovoy, *Phys. Rev. Lett.* **96**, 067601 (2006).
- [15] M. Mochizuki and N. Furukawa, *Phys. Rev. B* **80**, 134416 (2009).
- [16] R. Feyerherm, E. Dudzik, A. U. B. Wolter, S. Valencia, O. Prokhnenko, A. Maljuk, S. Landsgesell, N. Aliouane, L. Bouchenoire, S. Brown, and D. N. Argyriou, *Phys. Rev. B* **79**, 134426 (2009).
- [17] R. Feyerherm, E. Dudzik, O. Prokhnenko, and D. N. Argyriou, *J. Phys.: Conf. Ser.* **200**, 012032 (2010).
- [18] A. Skaugen, D. K. Shukla, R. Feyerherm, E. Dudzik, Z. Islam, and J. Stempfer, *J. Phys.: Conf. Ser.* **519**, 012007 (2014).
- [19] E. Schierle, V. Soltwisch, D. Schmitz, R. Feyerherm, A. Maljuk, F. Yokaichiya, D. N. Argyriou, and E. Weschke, *Phys. Rev. Lett.* **105**, 167207 (2010).
- [20] H. C. Walker, F. Fabrizi, L. Paolasini, F. de Bergevin, J. Herrero-Martin, A. T. Boothroyd, D. Prabhakaran, and D. F. McMorrow, *Science* **333**, 1273 (2011).
- [21] J. Hemberger, F. Schrettle, A. Pimenov, P. Lunkenheimer, V. Y. Ivanov, A. A. Mukhin, A. M. Balbashov, and A. Loidl, *Phys. Rev. B* **75**, 035118 (2007).
- [22] Y. Yamasaki, S. Miyasaka, T. Goto, H. Sagayama, T. Arima, and Y. Tokura, *Phys. Rev. B* **76**, 184418 (2007).
- [23] U. Englisch, H. Rossner, H. Maletta, J. Bahrtdt, S. Sasaki, F. Senf, K. Sawhney, and W. Gudat, *Nucl. Instrum. Methods Phys. Res., Sect. A* **467-468**, 541 (2001).
- [24] J. Fink, E. Schierle, E. Weschke, and J. Geck, *Rep. Prog. Phys.* **76**, 056502 (2013).

- [25] J. Stremper, S. Francoual, D. Reuther, D. K. Shukla, A. Skaugen, H. Schulte-Schrepping, T. Kracht, and H. Franz, *J. Synchrotron Radiat.* **20**, 541 (2013).
- [26] V. Y. Ivanov, A. A. Mukhin, V. D. Travkin, A. S. Prokhorov, Y. F. Popov, A. M. Kadamtseva, G. P. Vorob, K. I. Kamilov, and A. M. Balbashov, *Phys. Status Solidi B* **243**, 107 (2006).
- [27] J. P. Hill and D. F. McMorrow, *Acta Crystallogr. Sect. A: Found. Crystallogr.* **52**, 236 (1996).
- [28] H. Jang, J.-S. Lee, K.-T. Ko, W.-S. Noh, T. Y. Koo, J.-Y. Kim, K.-B. Lee, J.-H. Park, C. L. Zhang, S. B. Kim, and S.-W. Cheong, *Phys. Rev. Lett.* **106**, 047203 (2011).
- [29] D. Mannix, A. Stunault, N. Bernhoeft, L. Paolasini, G. H. Lander, C. Vettier, F. de Bergevin, D. Kaczorowski, and A. Czopnik, *Phys. Rev. Lett.* **86**, 4128 (2001).
- [30] T. A. W. Beale, S. B. Wilkins, R. D. Johnson, S. R. Bland, Y. Joly, T. R. Forrest, D. F. McMorrow, F. Yakhou, D. Prabhakaran, A. T. Boothroyd, and P. D. Hatton, *Phys. Rev. Lett.* **105**, 087203 (2010).
- [31] S. Partzsch, S. B. Wilkins, J. P. Hill, E. Schierle, E. Weschke, D. Souptel, B. Büchner, and J. Geck, *Phys. Rev. Lett.* **107**, 057201 (2011).
- [32] M. W. Haverkort, C. Schüßler-Langeheine, C. F. Chang, M. Buchholz, H.-H. Wu, H. Ott, E. Schierle, D. Schmitz, A. Tanaka, and L. H. Tjeng, [arXiv:0805.4341](https://arxiv.org/abs/0805.4341).
- [33] B. T. Thole, G. van der Laan, J. C. Fuggle, G. A. Sawatzky, R. C. Karnatak, and J.-M. Esteve, *Phys. Rev. B* **32**, 5107 (1985).
- [34] D. Mannix, D. F. McMorrow, R. A. Ewings, A. T. Boothroyd, D. Prabhakaran, Y. Joly, B. Janousova, C. Mazzoli, L. Paolasini, and S. B. Wilkins, *Phys. Rev. B* **76**, 184420 (2007).
- [35] T. R. Forrest, S. R. Bland, S. B. Wilkins, H. C. Walker, T. A. W. Beale, P. D. Hatton, D. Prabhakaran, A. T. Boothroyd, D. Mannix, F. Yakhou, and D. F. McMorrow, *J. Phys.: Condens. Matter* **20**, 422205 (2008).
- [36] L. Palermo and X. A. Da Silva, *Phys. Status Solidi B* **102**, 661 (1980).
- [37] H. Katsura, N. Nagaosa, and A. V. Balatsky, *Phys. Rev. Lett.* **95**, 057205 (2005).
- [38] I. A. Sergienko and E. Dagotto, *Phys. Rev. B* **73**, 094434 (2006).
- [39] N. Aliouane, O. Prokhnenko, R. Feyerherm, M. Mostovoy, J. Stremper, K. Habicht, K. C. Rule, E. Dudzik, A. U. B. Wolter, A. Maljuk, and D. N. Argyriou, *J. Phys.: Condens. Matter* **20**, 434215 (2008).
- [40] G. Khaliullin, *Phys. Rev. Lett.* **111**, 197201 (2013).